Journal of Photochemistry and Photobiology 12 (2022) 100158

Contents lists available at ScienceDirect

Journal of Photochemistry and Photobiology

journal homepage: www.sciencedirect.com/journal/journal-of-photochemistry-and-photobiology

Nicotinamide and calcipotriol counteract UVB-induced photoaging on primary human dermal fibroblasts

Lara Camillo [a], Laura Cristina Gironi [b], Elia Esposto [a], Elisa Zavattaro [b,c,*], Paola Savoia [a]

[a] Department of Health Sciences, University of Eastern Piedmont, Novara, Italy
[b] AOU Maggiore della Carità di Novara, Italy
[c] Department of Translational Medicine, University of Eastern Piedmont, Novara, Italy

ARTICLE INFO

Keywords:
Ultraviolet
Dermal fibroblasts
Photoaging
Nicotinamide
Calcipotriol
Senescence

ABSTRACT

Background: Photoaging is mainly caused by ultraviolet radiations inasmuch they can damage the DNA, trigger ROS production, and activate p53/p21 pathway, which cause cell cycle arrest and senescence. The accumulation of senescent cells within the dermis contributes to tissue deregulation and skin carcinogenesis. However, the use of photoprotector molecules could reduce UV-induced damages and prevent photoaging. Therefore, the aim of this study is to evaluate whether the active forms of vitamin B3 (nicotinamide) and the analog of vitamin D3 (calcipotriol) might protect primary human dermal fibroblasts (HDFs) from UVB-induced photoaging.
Methods: HDFs were isolated from a healthy adult donor and stimulated with nicotinamide (25 μM) and calcipotriol (100 nM) for 24h before UVB exposure, and then, cultured for further 24h on vitamin-supplemented media. Then, cell viability, ROS production, DNA damages, senescence markers, protein and gene expression were evaluated.
Results: HDFs treated with nicotinamide and calcipotriol showed better proliferation properties and lower DNA damages due to a reduced UVB-induced ROS production. Consequently, p53/p21 pathway was less active which enhanced cell cycle progression and reduced senescence and cell death.
Conclusions: Overall, our results suggest that nicotinamide and calcipotriol can counteract UVB-induced effects responsible for the onset of skin photoaging.

1. Introduction

Extrinsic aging also termed photoaging, is a cumulative process induced by sunlight exposure, in particular by ultraviolet (UV) radiations, that is also influenced by individual's lifestyle, skin phototype, and geographic location [1,2]. UVB (280-320 nm) is the main responsible for skin aging as their highly energetic rays are mostly absorbed by the epidermis and partially by the papillary dermis [3,4]. UVB can directly damage the DNA [5] and enhance the production of reactive oxygen species (ROS) [6], which in turn amplifies DNA oxidative damages, like the formation of 8-hydroxy-2'-deoxyguanine (8-OHdG) bases [7]. In presence of persistent DNA damage response (DDR) due to chronic UV exposure, cells permanently arrest the cell cycle through a dynamic multistage process known as senescence [8,9]. Cell growth arrest is controlled by the p53/p21 and/or p16/pRB pathways that inhibit cyclin-dependent kinases (CDKs) -2 and -4 respectively, blocking the cell cycle [8,10]. To repair oxidative DNA damages, senescent cells activate the base excision repair (BER) system, specifically the 8-oxoguanine DNA glycosylase (OGG1) enzyme, which removes 8-OHdG bases on the DNA [11]. Besides, senescent cells release senescence-associated secretory phenotype (SASP) molecules like proinflammatory cytokines, matrix metalloproteases (MMPs), and other chemokines [9,12,13]. Although this process is crucial for tumor suppression, the accumulation of senescent cells within tissues and the release of SASP molecules may contribute to neoplastic progression and aging [9,14]. Along with topical sunscreens, the use of molecules able to prevent/treat UV-induced damage at the molecular level has become a topic of increasing interest in recent years [15]. One of the main systemic supplements used is nicotinamide (NAM), the amide form of vitamin B3. It is the precursor of nicotinamide adenine dinucleotide (NAD) and shows an anti-aging activity favoring DNA repair and inhibiting the inflammatory response [16]. In our recent study [17], we proved that NAM (25 μM) given 24 hours before UVB exposure can efficiently prevent DNA damages and the oxidative stress outcome on human primary

* Corresponding author at: Department of Translational Medicine, University of Eastern Piedmont, Via Solaroli 17, 28100, Novara, Italy.
E-mail address: elisa.zavattaro@med.uniupo.it (E. Zavattaro).

https://doi.org/10.1016/j.jpap.2022.100158

Available online 21 November 2022
2666-4690/© 2022 Published by Elsevier B.V. This is an open access article under the CC BY-NC-ND license (http://creativecommons.org/licenses/by-nc-nd/4.0/).

keratinocytes. Although several studies have demonstrated the beneficial effects of NAM on irradiated fibroblasts [18], is not completely clear its role against UVB-induced senescence. Along with NAM, vitamin D3 has been suggested for photoprotection [19]. Vitamin D3 is a fat-soluble vitamin synthesized by keratinocytes when exposed to UV light. Due to its anti-inflammatory and anti-proliferative action, vitamin D3 is used for the treatment of various skin disorders [20], although few data are available on its role as a photoprotector. Due to their properties, together with their safety, reduced adverse effects, and low costs, vitamin B3 and D3 could be a useful weapon to counteract photoaging and prevent cancer development.

Considering that photoaging mainly affect adult patients, in this paper we chose to investigate the effects of vitamin B3 and D3 against UVB-induced damages on primary adult human dermal fibroblasts (HDFs), that we have choosen as the closest *in-vivo* model for this study.

2. Methods

2.1. Chemicals and reagents

Dulbecco's modified eagle medium (DMEM) high glucose, fetal bovine serum (FBS) and penicillin/streptomycin were purchased by Euroclone (Pero, Italy). Nicotinamide, calcipotriol, 3-(4,5-dimethylthiazol-2-yl)-2,5-diphenyltetrazolium bromide (MTT), DMSO, RIPA lysis buffer, 2x Loading buffer (LB), rabbit anti-phospho-p53 (Ser15), rabbit anti-p53, secondary HRP-conjugated anti-mouse and anti-rabbit antibodies were purchased by Sigma-Aldrich (St. Lois, MO, USA). RNAse A and propidium iodide (PI) were purchased by Immunological Sciences (Rome, Italy). Annexin V-FITC 500x, mouse anti-Ki67 and DCFDA-Cellular ROS assay kit were obtained from Abcam (Cambridge, UK). Primary rabbit anti-OGG1 and mouse anti-β-actin antibodies, Measure-IT High Sensitivity Nitrite Assay Kit, secondary antibody anti-mouse Alexa Fluor-546, anti-rabbit Alexa Fluor-488 antibody were purchased by Thermo Fisher (Waltham, MA, USA).

2.2. Human dermal fibroblasts isolation and culture

Primary HDFs were isolated from a healthy skin biopsy of a male donor (42 years old) as previously described [21], after obtained informed consent. HDFs were cultured in Dulbecco's modified eagle medium (DMEM) high glucose (Euroclone) containing 10% of fetal bovine serum (FBS) (Euroclone) and 1% of penicillin/streptomycin (Euroclone). HDFs were used from passage 5 to 11.

2.3. HDFs treatment

HDFs were treated with 25 μM nicotinamide (Sigma-Aldrich) and 100 nM calcipotriol (Sigma-Aldrich) [22], in DMEM 10% FBS for 24 h. Then, cells were washed and exposed with a tiny layer of PBS to 40 mJ/cm^2 UVB (280-320 nm) using a VL6M lamp (Montepaone, Torino, Italy) with a peak at 312 nm. The UV spectrum was measured with a quantum photo/radiometer (HD9021, Montepaone). PBS was removed and vitamins-supplemented cell media was added for 24 h.

2.4. MTT assay

HDFs (7×10^3 cells/well) were seeded into a 96-wells multiplate and treated as described above. After treatment, 0.2 mg/ml of MTT (Sigma-Aldrich) were added and formazan crystal were dissolved with DMSO (Sigma-Aldrich). Absorbance was read at 570 nm using Victor X Multilabel Plate Readers (PerkinElmer, Milano, Italy).

2.5. Cell cycle analysis by flow cytometry

HDFs (4×10^5 cells/well) were seeded into a 6-wells multiplate and treated as described above. Then, medium with apoptotic cells was collected, and cells were detached through trypsinization, centrifuged, fixed with cold ethanol 70%, and incubated for 1 h at -20°C. Cells were washed twice and resuspended in 200 μl PBS with 25 μg/ml RNAse A (Immunological Sciences) and 100 μg/ml propidium iodide (PI) (Immunological Sciences) and incubated for 15 min at 37 °C protected from light. Cell cycle was analyzed with Attune NxT FACS (Thermo Fisher).

2.6. Annexin V/PI flow cytometry assay

HDFs (1×10^5 cells/well) were plated into a 6-wells multiplate and treated as described above. Cells were detached by trypsinization, centrifuged, and resuspended into 250 μl of binding buffer. Then 1 μl of Annexin V-FITC 500x (Abcam) and 1 μl of PI (Abcam) were added to cell suspension and incubated 15 min at RT. Fluorescence was analyzed with Attune NxT FACS (Thermo Fisher).

2.7. Single cell gel electrophoresis

DNA fragmentation was evaluated through comet assay as previously described [17]. Briefly, HDFs (2×10^5 cells/well) were plated into a 6-wells multiplate and treated as described above. Cells were detached through trypsinization and resuspended in 1% low melting agarose (Fisher Molecular Biology, Trevose, PA, USA) and solidified on pre-coated microscope slides. Then, cells were incubated in lysis buffer overnight at 4 °C. After electrophoresis in the appropriate buffer, slides were stained with 10 μg/ml of propidium iodide per 20 min protected from light. Pictures of cells were taken using a fluorescence microscope Leica DS5500B (Leica Microsystems) and quantification of the tail DNA % was performed using the automated CometScore 2.0 software (TriTek).

2.8. Intracellular ROS quantification

Intracellular ROS quantification was performed using the DCFDA-Cellular ROS assay kit (Abcam) following the manufacturer's instructions. HDFs (2.5×10^4 cells/well) were seeded into a 96-wells microplate and treated as described above. Then, cells were washed twice with PBS and incubated for 45 minutes at 37 °C with 10 μM DCFDA solution. The probe was replaced with fresh PBS and the fluorescence was read with Victor X Multilabel Plate Readers (PerkinElmer) at 495/529 nm excitation/emission.

2.9. Quantitative real-time reverse transcriptase-PCR (qRT-PCR)

HDFs (4×10^5 cells/well) were plated into a 6-wells microplate and treated as described above. Cells were detached mechanically and resuspended in 500 μl of Trizol for the total RNA isolation. The amount and purity of RNA were quantified at the spectrophotometer (Nanodrop, Thermo Fisher) by measuring the optical density at 260 and 280 nm. Reverse transcriptase was performed using a high-capacity cDNA reverse transcription kit (Applied Biosystems, Foster City, California, USA) according to the manufacturer's instructions. A two-step cycling qRT-PCR was performed in a volume of 10 μl per well in a Multiply Optical Strip (Sarstedt, Nümbrecht, Germany) containing SensiFast SYBR No-ROX kit (Bioline, London, UK), forward and reverse primer 400 nM, and 1 μl of cDNA template. Primers used are indicated in **Table S1**. GAPDH was used for data normalization and the relative quantification was determined by the $2^{\Delta CT}$ method. Data are expressed as fold change versus CTRL cells ($2^{-\Delta\Delta CT}$).

2.10. Senescence-associated β-galactosidase staining

HDFs (5×10^4 cells/well) were seeded into a 6-wells multiplate and treated as previously described. Senescence-associated β-galactosidase (SA-β-gal) staining was performed using the Senescence β-galactosidase

Staining Kit (Cell Signaling Technology, Danvers, MA, USA) following manufacturer's instructions. Briefly, cells were washed twice in PBS and fixed using Fixative Solution for 15 minutes at RT. Cells were washed twice with PBS and incubated with β-Galactosidase Staining Solution overnight at 37 °C. Cells were checked and photographed using light inverted microscope Leica DMi1 (Leica Microsystems). At least 3 different pictures were taken of the same sample. SA-β-GAL percentage positive cells was quantified with ImageJ software [23] (http://imagej.net, RRID: SCR_003070).

2.11. Western blotting

HDFs (2×10^5 cells/well) were seeded into a 6-wells multiplate and treated as described above. Cells were homogenized in cold RIPA lysis buffer (Sigma-Aldrich) supplemented with protease inhibitor cocktail (Thermo Fisher) and phosphatase inhibitors. Proteins were quantified by BCA assay (Thermo Fisher) and denaturated in 2x LB (Sigma-Aldrich) at 95 °C for 5 min. 40 μg of proteins were loaded on 10% acrylamide SDS-PAGE gel. Proteins were transferred to PVDF membrane (Biorad) and incubated with primary antibodies rabbit anti-OGG1 (Thermo Fisher, cat# PA5-98026, RRID AB_2812640, 1:1000), rabbit anti-phospho-p53 (Ser15) (Sigma-Aldrich, cat# SAB4504499, 1:500) and rabbit anti-p53 (Sigma-Aldrich, cat# SAB5700047, 1:1000) overnight at 4 °C. Secondary antibodies HRP-conjugated anti-mouse (Sigma-Aldrich, cat# AP181P, 1:10.000) and anti-rabbit (Sigma-Aldrich, cat# A9169, 1:12.000) were added for 45 minutes at RT. Antibody mouse β-actin (Thermo Fisher, cat# MA1-140, RRID: AB_2536844, 1:5000) was used as homogenate protein loading control. Membranes were developed using enhanced chemiluminescence method (ECL, Biorad, Hercules, CA, USA) and acquired with ChemiDoc Imaging System (Biorad). The relative band intensity was quantified using ImageJ Software [23]. Densiometric analysis data are expressed as protein/β-actin ratio.

2.12. Intracellular nitric oxide

Intracellular nitrate quantification was performed using Measure-IT High Sensitivity Nitrite Assay Kit (Thermo Fisher) following the manufacturer's instruction. HDFs (4×10^4 cells/well) were plated into a 24-wells microplate and were treated as previously described. Cells were washed and lysed with 200 μl of double distilled water. Meanwhile, a 96-well microplate was prepared with 100 μl of working solution, and 10 μl of cell supernatant was added and incubated at RT for 10 minutes. 5 μl of quantification developer were added to each well and the plate was read at 365/450 nm excitation/emission using Victor X Multilabel Plate Readers (PerkinElmer).

2.13. Indirect immunofluorescence

HDFs (1×10^4 cells/well) were seeded on rounded sterile glasses and treated as described above. Cells were washed and fixed with 4% paraformaldehyde at 4 °C for 10 minutes. Then, cells were incubated with blocking buffer for 1 h at RT. Primary antibodies mouse anti-Ki67 (Abcam, cat# ab819, 1:50) and rabbit anti-p21 (Sigma-Aldrich, cat# SAB1306168, 1:300), diluted in PBS + 0.1% Triton + 2% BSA, were added to samples for 2 h at RT. Cells were incubated with secondary antibody anti-mouse Alexa Fluor-546 (Thermo Fisher) and anti-rabbit Alexa Fluor-488 (Thermo Fisher) added with DAPI (1:1000, Sigma-Aldrich) for 45 minutes at RT and mounted with glycerol. Pictures were taken with an optical fluorescent microscope Leica DS5500B (Leica Microsystems, Inc., Buffalo Grove, IL); quantification was performed using the ImageJ Software [23]. p21 expression was measured on at least 50 cells from three different pictures of three independent experiments and expressed as corrected total cell fluorescence (CTCF) calculated with the formula: integrated density- (area of selected cell * mean fluorescence of backgrounds). Ki67 percentage score was defined as the percentage of positively stained cells among the total number of cells assessed.

2.14. Statistical analysis

Statistical analysis was performed using GraphPad Prism version 8 (California, USA; http://www.graphpad.com, RRID: SCR_002798). Data were expressed as mean ± SEM of *n* independent experiments. Statistical significance was assessed by Student's t-test for different groups of treatment comparisons. Statistical significance was defined as $p < 0.05$.

3. Results

3.1. Cell proliferation and cell viability on irradiated HDFs

We carried out a preliminary experiment, stimulating the HDFs with NAM and CAL to exclude any negative effect on cell viability. The results are presented as supplementary material (Figure S1A): notably, none of the vitamins reduced the cells viability.

Then, since UVB can inhibit cell proliferation [24], we analyzed Ki67 expression through indirect immunofluorescence performed on irradiated HDFs (Fig. 1A). As expected, UVB significantly lowered the percentage of cells expressing Ki67 (Fig. 1B). However, treatment with NAM and CAL reverted this trend, improving cell proliferation. We also tested cell viability (Fig. 1C) which was affected after UVB exposure with no improvements obtainable with both vitamins.

3.2. Vitamins reduce UV-induced oxidative stress

Since oxidative stress is considered the primary mechanism of photoaging [1], we firstly quantified ROS production on both unirradiated and irradiated HDFs. Vitamins alone did not show any modulation on basal ROS production (Figure S1B). However, after irradiation (Fig. 2A), ROS levels were significantly higher compared to control cells; both NAM and CAL treatment prevented this phenomenon. Consistently, we found increased *SOD-1* mRNA expression (Fig. 2B) after UVB exposure but lower levels in presence of NAM. Finally, we tested *MMP-1* gene expression (Fig. 2C), normally released after AP-1 activation induced by ROS [2]. Again, upon irradiation we found higher levels of *MMP-1* expression, efficiently reduce by NAM and CAL. These results suggest that vitamins might prevent oxidative stress and ROS release induced by UV.

3.3. Effects of vitamins on oxidative DNA damage repair

Both UV rays and ROS can damage the DNA [25]. Since HDFs treated with vitamins showed reduced ROS levels and oxidative stress markers expression, we investigated whether also DNA damages were prevented by vitamins treatment by evaluating DNA fragmentation, through comet assay (Fig. 3A), and the quantification of OGG1 expression as a marker of oxidative DNA damage. Consistently, irradiated HDFs treated with NAM and CAL showed less DNA fragmentation compared to UVB-treated cells (Fig. 3B), which correlated with a reduced *OGG1* gene (Figs. 3C) and protein (Fig. 3D) expression. These results may suggest that vitamins, in particular NAM and CAL, can prevent oxidative DNA damages.

3.4. Vitamins lowered p53/p21 pathway UVB-induced

To repair oxidative DNA damages, cells activate the p53/p21 growth-suppressive pathway which leads to cell cycle arrest and senescence [26], through p53 activation via phosphorylation (p-p53) on Ser15 that in turn regulates p21 expression [12]. Considering that NAM and CAL treatments showed lower oxidative stress and DNA damages, we investigated whether with these results might correlate a reduced p53/p21 activation. Indeed, we found that *p53* gene expression (Fig. 4A) was increased after UVB exposure, but vitamin treatments efficiently

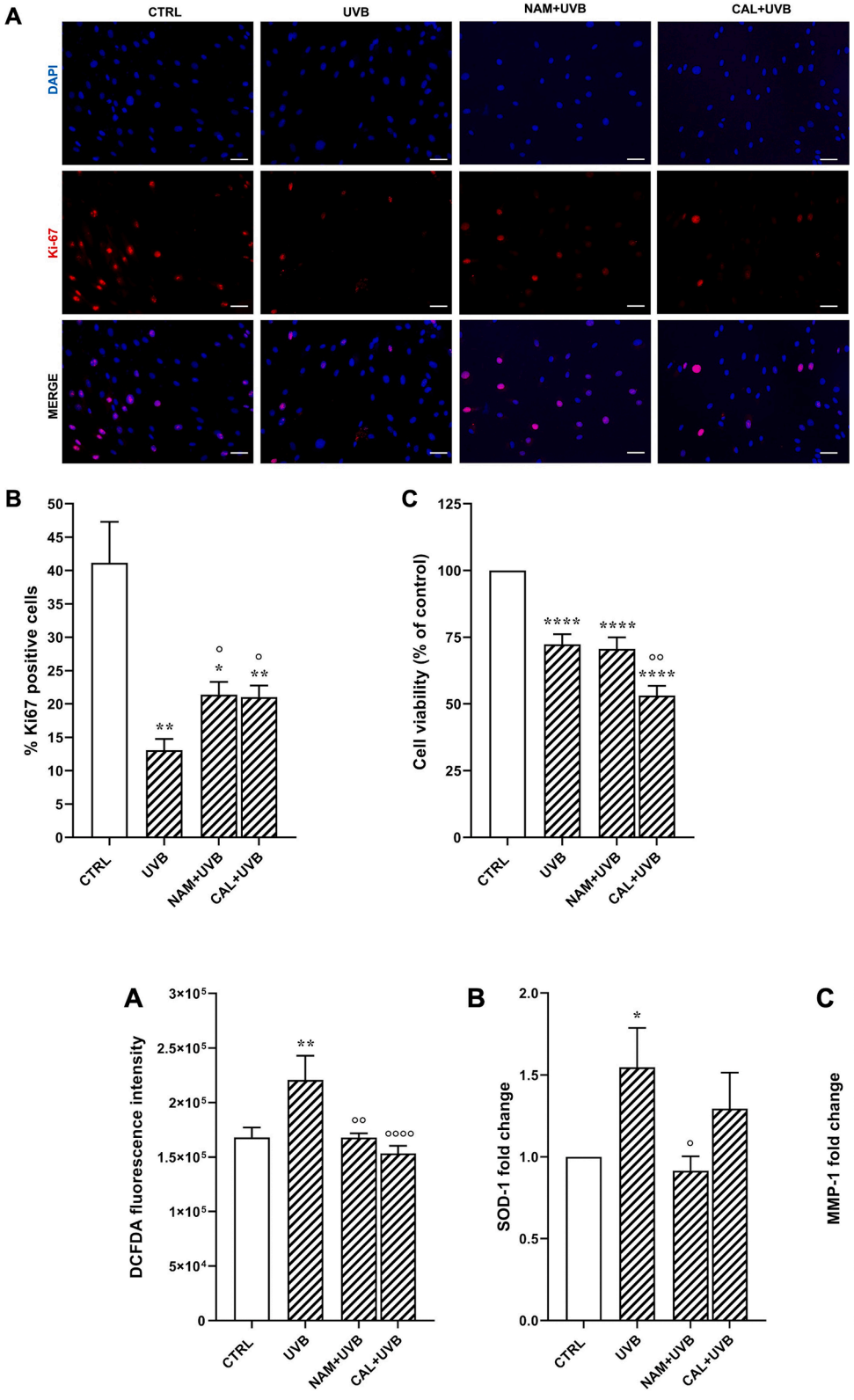

Fig. 1. Effects cell proliferation and viability. HDFs were stimulated with NAM (25 μM) and CAL (100 nM) for 24h, irradiated with UVB 40 mJ/cm^2, and incubated for 24 h. **(A)** Representative IF of Ki67 and **(B)** percentage of Ki67 positive cells of three independent experiments indicated as means ± SEM. **(C)** MTT assay for evaluation of cell viability expressed as means ± SEM of seven independent experiments. *p <0.05, **p<0.01, ****p<0.0001 vs CTRL; °p<0.05, °°p<0.01 vs UVB. CTRL, untreated cells; NAM, nicotinamide; CAL, calcipotriol.

Fig. 2. Vitamins reduced ROS production and oxidative stress markers expression. HDFs were stimulated with NAM (25 μM) and CAL (100 nM) for 24h, irradiated with UVB 40 mJ/cm^2, and incubated for 24 h. **(A)** Intracellular ROS quantification using DCFDA fluorescent probe. Data are expressed as means ± SEM of four independent experiments. **(B)** Gene expression of *SOD-1* and **(C)** *MMP-1*. Data are expressed as means ± SEM of seven independent experiments. *p <0.05, **p<0.01, vs CTRL; °p<0.05, °°p<0.01, °°°°p<0.0001 vs UVB. CTRL, untreated cells; NAM, nicotinamide; CAL, calcipotriol.

reverted this trend. Similarly, we found higher levels of p-p53 (Figs. 4B-C) on UVB irradiated HDFs, which were slightly lower in presence of vitamins. Conversely, NAM-treated cells presented higher p53 levels compared with control cells (Figs. 4B, D). In line with these results, we found that p21 gene (Fig. 4E) and protein (Figs. 4F, G) expression was significantly higher in comparison with control cells

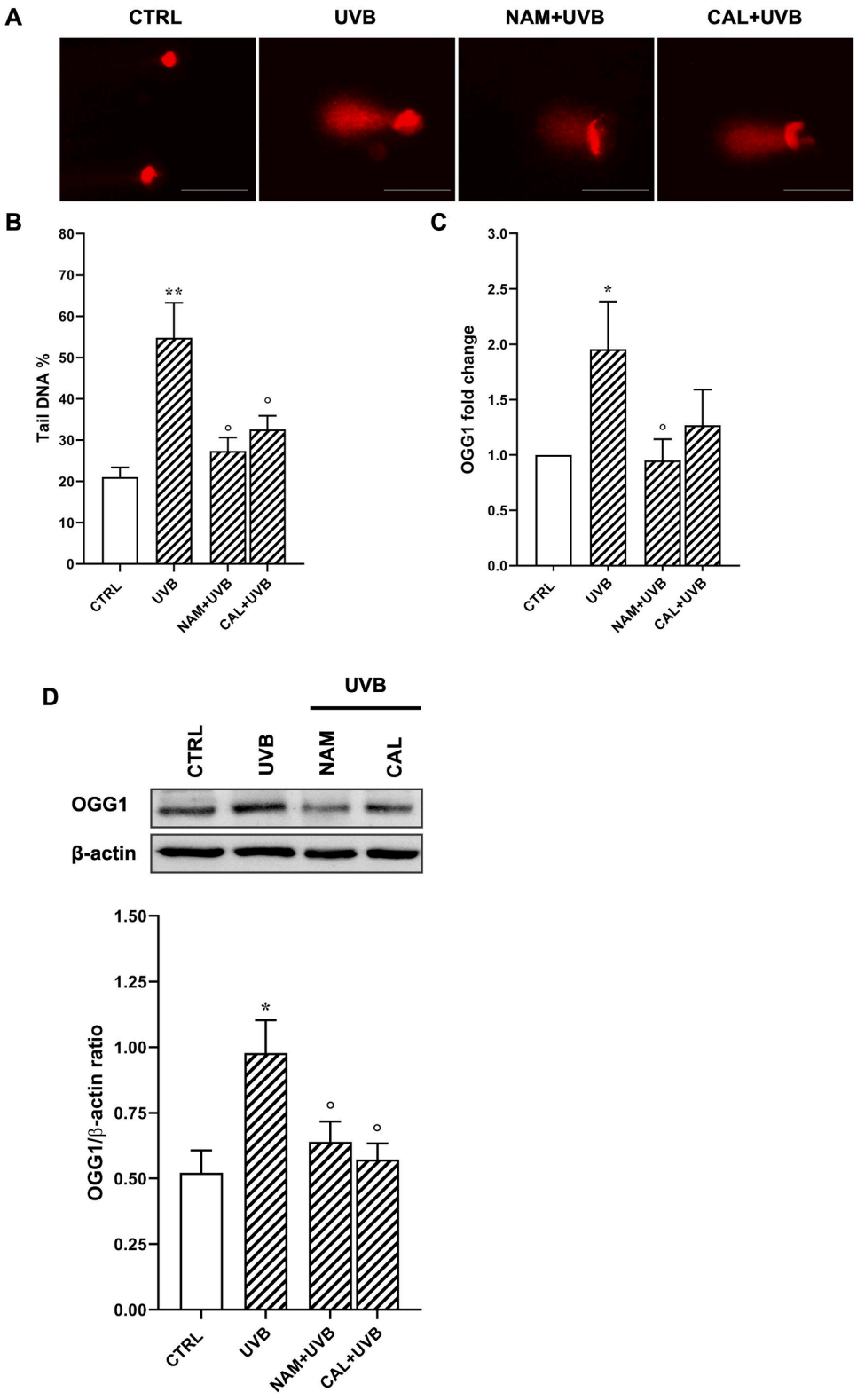

Fig. 3. Vitamins reduced DNA damages and OGG1 expression. HDFs were stimulated with NAM (25 μM) and CAL (100 nM) for 24h, irradiated with UVB 40 mJ/cm^2, and incubated for 24 h. **(A)** Representative comet assay and **(B)** tail DNA % quantification of six independent experiments expressed as means ± SEM. **(C)** *OGG1* gene expression expressed as means ± SEM of seven independent experiments. **(D)** Representative western blotting and densiometric analysis of OGG1 protein expression vs β-actin expression represented as means ± SEM of six independent experiments. *p<0.05, **p<0.01 vs CTRL; °p<0.05 vs UVB. CTRL, untreated cells; NAM, nicotinamide; CAL, calcipotriol.

while treatment with vitamins lowered p21 gene and protein expression. These results suggest that UVB-induced DNA damages induce the activation of p53 and, consequently, p21 transcription. However, with reduced DNA damages due to NAM and CAL treatment, p53 is less active and p21 expression is lowered.

3.5. Vitamins restored cell cycle and reduced senescence on irradiated HDFs

As a result of UVB-mediated p53/p21 pathway activation, the cell cycle is arrested. Therefore, we investigated whether the decreased activation of the p53/p21 pathway mediated by vitamins correlates with improved cell cycle and reduced senescence. Firstly, we analyzed the

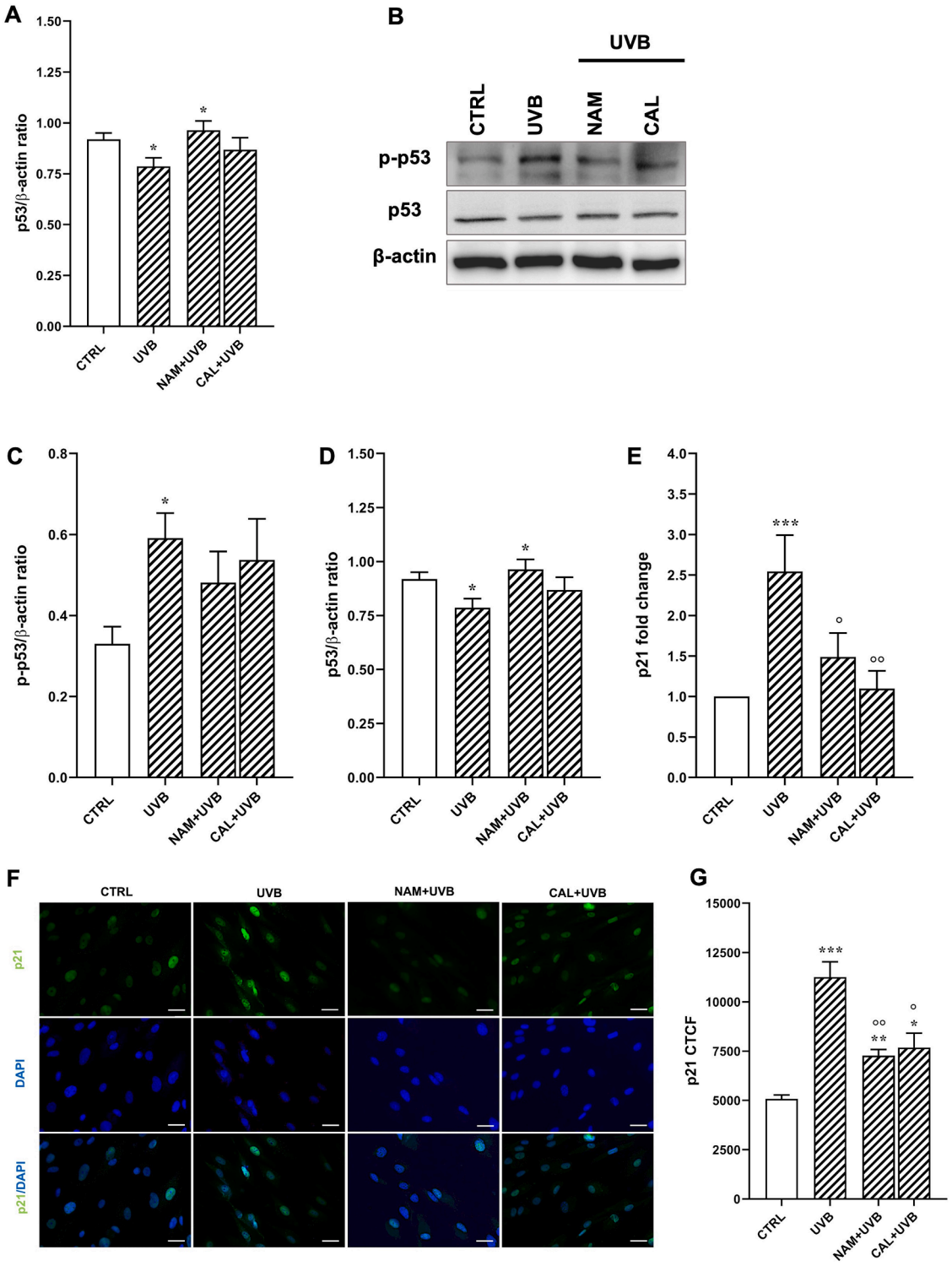

Fig. 4. Vitamins reduced the activation of p53/p21 pathway. (A) *p53* gene expression of seven independent experiments indicated as means ± SEM. **(B)** Representatives western blotting of p-p53 and p53 protein expression. Densiometric analysis of p-p53 **(C)** and p53 **(D)** is represented as means ± SEM of five independent experiments expressed as p-p53/β-actin ratio and p-53/β-actin ratio. **(E)** *p21* gene expression expressed as means ± SEM of seven independent experiments. **(F)** Representative IF of p21 stain and **(G)** p21 IF quantification with though CTCF. Data are indicated as means ± SEM of four independent experiments. At least 50 cells were measured for each experiment. *p<0.05, **p<0.01, ***p<0.001 vs CTRL; °p<0.05, °°p<0.01 vs UVB. CTRL, untreated cells; NAM, nicotinamide; CAL, calcipotriol; CTCF, corrected total cell fluorescence.

cell cycle phases through propidium iodide stain using flow cytometry as shown on Fig. 5A and Figure S2. UVB significantly reduced the number of cells on the G2 phase in comparison with control cells (Fig. 5B), probably because of the upregulation of p21. On the other hand, vitamins, in particular NAM, showed an increased number of cells in the G2 phase, which correlates with the reduced level of p21 expression (Fig. 5B). We also evaluated the Sub-G1 phase (apoptotic cells) (Fig. 5C), and we found that the percentage of cells within this cell cycle phase was

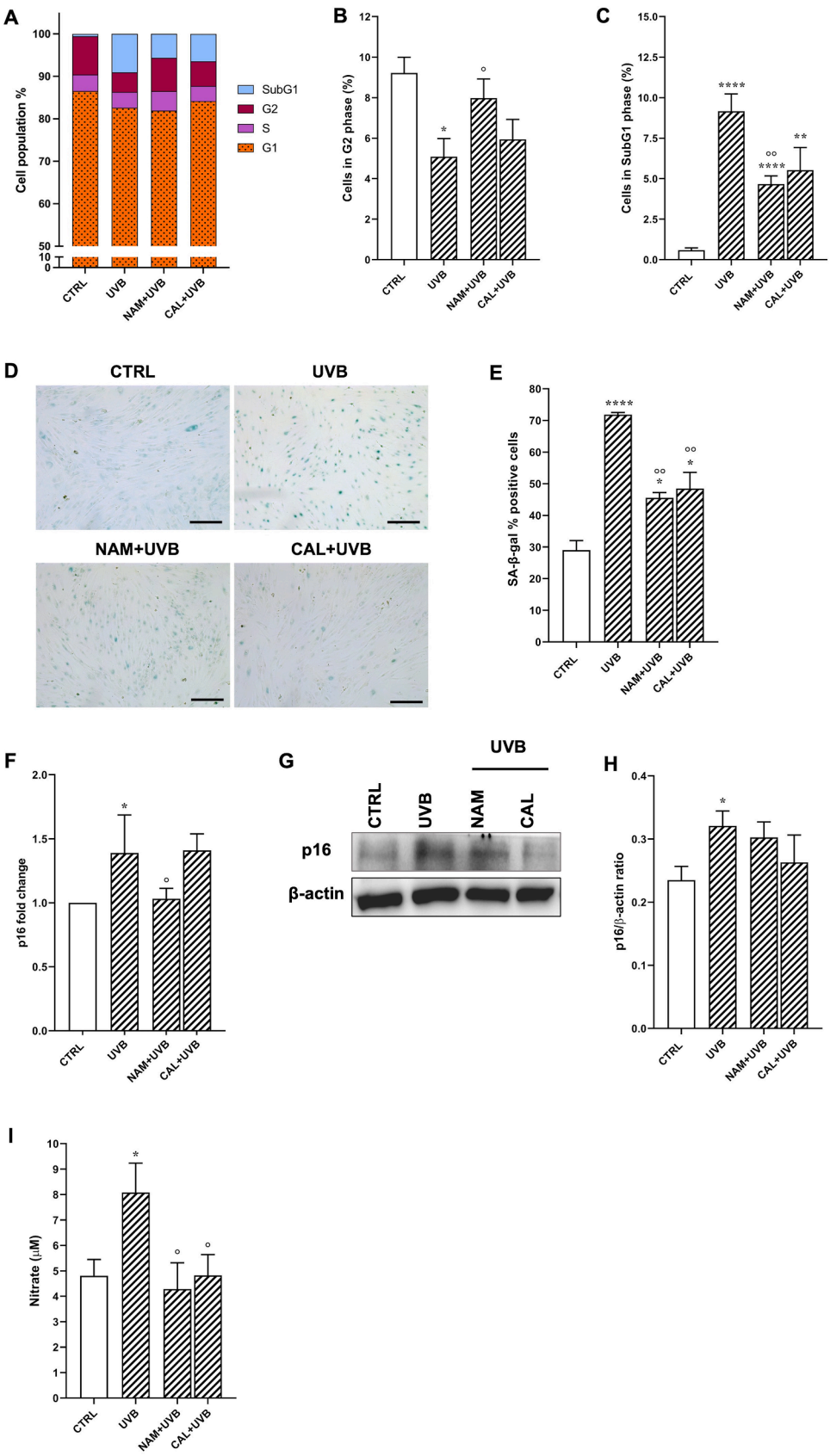

Fig. 5. Vitamin reduced cell cycle arrest and senescence. HDFs were stimulated with NAM (25 μM) and CAL (100 nM) for 24 h, irradiated with UVB 40 mJ/cm2 and incubated for 24 h. **(A)** Quantitative measurement of cell cycle phases. **(B)** Percentage of cells on G2 phase and **(C)** on Sub-G1 phase. Data are expressed as means ± SEM of seven independent experiments. **(D)** Representative SA-β-gal stain and **(E)** and percentage of SA-β-gal positive cells. Data are expressed as means ± SEM of four independent experiments. **(F)** *p16* gene expression of seven independent experiments expressed as means ± SEM. **(G)** Representative western blotting and **(H)** densiometric analysis of six independent experiments expressed as means ± SEM. **(I)** Intracellular nitrate concentration expressed as means ± SEM of six independent experiments. *p<0.05, ****p<0.0001 vs CTRL; °p<0.05, °°p<0.01 vs UVB. CTRL, untreated cells; NAM, nicotinamide; CAL, calcipotriol.

15-fold higher after UVB irradiation, but both NAM and CAL reverted this trend. We further investigated in which apoptosis stage were cells found into the Sub-G1 phase using annexin V-FITC / PI staining and analyzed with flow cytometry (Figure S2A, B). Interestingly, we found that UVB induced early apoptosis, which was slightly reverted by vitamins. These results suggest that vitamins could restore the cell cycle and reduce cell death.

Due to the activation of the p53/p21 pathway and cell cycle arrest, cells undergo senescence. Hence, we first analyzed the expression of SA-β-gal (Fig. 5) as marker of lysosomal activity. As shown in Fig. 5E, after UVB irradiation the number of cells expressing SA-β-gal was significantly higher compared with control cells. Nevertheless, cells treated with vitamins were less positive to the SA-β-gal stain, suggesting that vitamins could prevent senescence. Secondly, we quantified p16 expression as a marker of senescence and cell cycle arrest. As expected, UVB irradiation significantly increased *p16* gene (Fig. 5F) and protein expression (Fig. 5G-H); however, only NAM treatment showed a significant reduction only on *p16* gene expression. Finally, we indirectly assessed the NO production through the quantification of nitrate (NO_2) as part of the SASP molecules (Fig. 5I) [27]. We found that NAM and CAL significantly reduced NO production on irradiated HDFs, which correlated with lower level of SA-β-gal and p16 expression. Therefore, these results confirm that with reduced p53/p21 activation, induced by NAM and CAL, cell cycle is restored, and senescence is inhibited.

4. Discussion

Photoaging is a premature skin aging due to chronic exposure to UV radiations, mainly UVB, affecting skin appearance and connective tissue functions [28]. UVB induces premature senescence, a permanent state of cell cycle arrest controlled by p53/p21 and p16/Rb pathways, as shown in Figure S4 [12]. The accumulation of senescent cells within the dermis can alter the connective tissue integrity and contribute to cancer development, due to the release of SASP molecules [10]. However, it has been proved that the use of photoprotective molecules could contribute to the prevention of photoaging and to the reduction of skin cancer onset [16]. For this reason, in our study we investigated the putative role of nicotinamide and calcipotriol (the active forms of vitamins B3 and D3, respectively), in the prevention of photoaging on dermal fibroblast, deepening the possible pathways involved. We think that our study model, consisting of adult HDFs, can adequately represent a closest *in-vivo* model of photoaging.

In this study, we demonstrated that vitamin B3 and D3 in their active form can protect cells from UVB-induced damage preventing senescence and photoaging.

Firstly, we observed that NAM and CAL treatments improved cell proliferation but only CAL restored cell viability after UVB exposure. Then, we evaluated ROS production and oxidative stress markers since oxidative stress is considered one of the initiators of photoaging [29]. We observed that after UVB exposure ROS production, antioxidant *SOD-1,* and oxidative stress marker *MMP*-1 gene expression were significantly higher compared to untreated cells, whereas NAM and CAL treatment reverted this trend. These results suggest that both vitamins have antioxidant activity and, especially for NAM, are in line with the results obtained in our previous work [17]. We hypothesized that both NAM and CAL have potentially antioxidant activity, although the mechanisms behind this phenomenon have yet to be clarified.

Next, we evaluated oxidative DNA damages and OGG1 expression, as a marker of BER activation. We found that cells treated with NAM and CAL presented fewer DNA damages and lower OGG1 expression in comparison with UVB-irradiated HDFs, in which DNA was acutely damaged. These results correlate with the reduced ROS production elicited by vitamins and may support our hypothesis of a vitamin-antioxidant activity. Subsequently, we evaluated the activation of the p53/p21 pathway as a response to DNA damage [12]. Consistently, we observed that UVB exposure increased the expression of p53 mostly found in the phosphorylated form. Moreover, we detected an increased p21 gene and protein expression, suggesting that the UV-induced DNA damages triggered the activation of p53, which in turn induced the transcription of p21, blocking the cell cycle and allowing DNA repair [30]. On the other hand, HDFs treated with vitamins showed a reduced p53 gene expression and activation, and consequently, lower levels of p21 expression. These results correlate with the reduced oxidative stress and DNA damages observed so far. To confirm these data, we analyzed cell cycle phases. We observed that the activation of p53 and p21 after UVB exposure correlates with the block of the cell cycle in the G2 phase and an increased percentage of cells into SubG1 phase. These data are in line with those reported by Greussing *et al* [31] which proved that the p53/p21 pathway was activated by UVB irradiation on HDFs. Nevertheless, NAM and CAL treatment showed an increased number of cells into G2 phase and a reduced percentage of apoptosis. This phenomenon could be due to the reduced p21 expression observed on NAM and CAL-treated HDFs along with decreased oxidative stress and DNA damages.

Finally, we evaluated senescence activation as a consequence of permanent cell cycle arrest. We found that irradiated HDFs, in comparison with vitamin-treated cells, showed an increased production of SA-β-gal, higher levels of p16 gene and protein expression and NO production, which was mostly reduced by NAM treatment.

5. Conclusions

Taken all together, these results might confirm our hypothesis that through an antioxidant activity, NAM and CAL prevent photoaging by reducing ROS release and consequently oxidative DNA damages, avoiding senescence, and reducing apoptosis. Therefore, our findings propound NAM and CAL as useful molecules for the prevention and treatment of photoaging. Their clinical safety and cost-effectiveness could potentially make them worldwide available strategies for reducing the incidence of skin cancer. However, more extensive studies are needed to better elucidate the mechanisms of action of these molecules, their possible synergy and their efficacy also in a clinical setting.

Fundings

This research did not receive any specific grant from funding agencies in the public, commercial, or not-for-profit sectors.

CRediT authorship contribution statement

Lara Camillo: Conceptualization, Data curation, Formal analysis, Investigation, Methodology, Resources, Validation, Visualization, Writing – original draft, Writing – review & editing. **Laura Cristina Gironi:** Conceptualization, Data curation, Formal analysis, Investigation, Validation, Visualization, Writing – review & editing. **Elia Esposto:** Data curation, Formal analysis, Investigation, Validation. **Elisa Zavattaro:** Data curation, Formal analysis, Investigation, Validation. **Paola Savoia:** Conceptualization, Funding acquisition, Investigation, Methodology, Project administration, Resources, Supervision, Validation, Writing – original draft, Writing – review & editing.

Declaration of Competing Interest

The authors declare that they have no known competing financial interests or personal relationships that could have appeared to influence the work reported in this paper.

Data availability

Data will be made available on request.

Acknowledgements

None.

Supplementary materials

Supplementary material associated with this article can be found, in the online version, at doi:10.1016/j.jpap.2022.100158.

References

[1] G.J. Fisher, S. Kang, J. Varani, et al., Mechanisms of photoaging and chronological skin aging, Arch. Dermatol. 138 (2002 Nov) 1462–1470.
[2] Han, A. Chien, A.L. Kang, S. Photoaging. Dermatol. Clin. 32 (2014 Jul) 291-9, vii. doi: 10.1016/j.det.2014.03.015.
[3] E. Fitsiou, T. Pulido, J. Campisi, F. Alimirah, M. Demaria, Cellular senescence and the senescence-associated secretory phenotype as drivers of skin photoaging, J. Invest. Dermatol. 141 (2021 Apr) 1119–1126.
[4] J.E. Sanches Silveira, D.M. Myaki Pedroso, UV light and skin aging, Rev. Environ. Health. 29 (2014) 243–254.
[5] C.A. Elmets, M. Athar, Milestones in photocarcinogenesis, J. Invest. Dermatol. 133 (2013 Jul 1) E13–E17.
[6] V.T. Natarajan, P. Ganju, A. Ramkumar, R. Grover, R.S. Gokhale, Multifaceted pathways protect human skin from UV radiation, Nat. Chem. Biol. 10 (2014 Jul) 542–551.
[7] J.E. Klaunig, Oxidative stress and cancer, Curr. Pharm. Des. 24 (2018) 4771–4778.
[8] N. Herranz, J. Gil, Mechanisms and functions of cellular senescence, J. Clin. Invest. 128 (2018 Apr 2) 1238–1246.
[9] J. Campisi, Cellular senescence: putting the paradoxes in perspective, Curr. Opin. Genet. Dev. 21 (2011 Feb) 107–112.
[10] A. Hernandez-Segura, J. Nehme, M. Demaria, Hallmarks of cellular senescence, Trends Cell. Biol. 28 (2018 Jun) 436) 453.
[11] M. Ichihashi, M. Ueda, A. Budiyanto, T. Bito, M. Oka, M. Fukunaga, K. Tsuru, T. Horikawa, UV-induced skin damage, Toxicology 189 (2003 Jul 15) 21–39.
[12] M. Cavinato, P. Jansen-Dürr, Molecular mechanisms of UVB-induced senescence of dermal fibroblasts and its relevance for photoaging of the human skin, Exp. Gerontol. 94 (2017 Aug) 78–82.
[13] N. Bhatia-Dey, R.R. Kanherkar, S.E. Stair, E.O. Makarev, A.B. Csoka, Cellular senescence as the causal nexus of aging, Front. Genet. 12 (2016 Feb) 13.
[14] J.P. Coppé, P.Y. Desprez, A. Krtolica, J. Campisi, The senescence-associated secretory phenotype: the dark side of tumor suppression, Ann. Rev. Pathol. 5. (2010) 99–118.
[15] T. Searle, F.R. Ali, F. Al-Niaimi, Systemic photoprotection in 2021, Clin. Exp. Dermatol. 46 (2021 Oct) 1189–1204.
[16] V.A. Snaidr, D.L. Damian, G.M. Halliday, Nicotinamide for photoprotection and skin cancer chemoprevention: A review of efficacy and safety, Exp. Dermatol. 28 (Suppl 1) (2019 Feb) 15–22.
[17] L. Camillo, L.C. Gironi, E. Zavattaro, E. Esposto, P. Savoia, Nicotinamide attenuates UV-induced stress damage in human primary keratinocytes from cancerization fields, J. Invest. Dermatol. 142 (2022 May) 1466–1477, e1.
[18] J.E. Oblong, The evolving role of the NAD+/nicotinamide metabolome in skin homeostasis, cellular bioenergetics, and aging, DNA Repair (Amst) 23 (2014 Nov) 59–63.
[19] C. Pihl, K. Togsverd-Bo, F. Andersen, M. Haedersdal, P. Bjerring, C.M. Lerche, Keratinocyte carcinoma and photoprevention: the protective actions of repurposed pharmaceuticals, phytochemicals and vitamins, Cancers (Basel) 13 (2021 Jul 22) 3684.
[20] M. Shahriari, P.E. Kerr, K. Slade, J.E. Grant-Kels, Vitamin D and the skin, Clin. Dermatol. 28 (2010 Nov-Dec) 663–668.
[21] L. Camillo, E. Grossini, S. Farruggio, L.C. Gironi, E. Zavattaro, P. Savoia, et al., Alpha-tocopherol protects human dermal fibroblasts by modulating nitric oxide release, mitochondrial function, redox status, and inflammation, Skin. Pharmacol. Physiol. 35 (2022) 1–12.
[22] H. Norsgaard, S. Kurdykowski, P. Descargues, T. Gonzalez, T. Marstrand, G. Dünstl, et al., Calcipotriol counteracts betamethasone-induced decrease in extracellular matrix components related to skin atrophy, Arch. Dermatol. Res. 306 (2014 Oct) 719–729.
[23] C.A. Schneider, W.S. Rasband, K.W. Eliceiri, NIH Image to ImageJ: 25 years of image analysis, Nat. Meth. 9 (2012) 671–675.
[24] A.J. Granados-López, E. Manzanares-Acuña, Y. López-Hernández, J.E. Castañeda-Delgado, I. Fraire-Soto, C.A. Reyes-Estrada, et al., UVB inhibits proliferation, cell cycle and induces apoptosis via p53, E2F1 and microtubules system in cervical cancer cell lines, Int. J. Mol. Sci. 22 (2021 May 14) 5197.
[25] E. Pelle, X. Huang, T. Mammone, K. Marenus, D. Maes, K. Frenkel, Ultraviolet-B-induced oxidative DNA base damage in primary normal human epidermal keratinocytes and inhibition by a hydroxyl radical scavenger, J. Invest. Dermatol. 121 (2003 Jul) 177–183.
[26] A. Karimian, Y. Ahmadi, B. Yousefi, Multiple functions of p21 in cell cycle, apoptosis and transcriptional regulation after DNA damage, DNA Repair (Amst) 42 (2016 Jun) 63–71.
[27] N Mabrouk, S Ghione, V Laurens, S Plenchette, A Bettaieb, C. Paul, Senescence and cancer: role of nitric oxide (NO) in SASP, Cancers (Basel) 12 (5) (2020 May 2) 1145.
[28] B.A.Photoaging Gilchrest, J. Invest. Dermatol. 133 (2013 Jul 1) E2–E6.
[29] C. Bilaç, M.T. Şahin, S. Öztürkcan, Chronic actinic damage of facial skin, Clin. Dermatol. 32 (2014 Nov-Dec) 752–762.
[30] S.L. Harris, A.J. Levine, The p53 pathway: positive and negative feedback loops, Oncogene 24 (2005 Apr 18) 2899–2908.
[31] R. Greussing, M. Hackl, P. Charoentong, et al., Identification of microRNA-mRNA functional interactions in UVB-induced senescence of human diploid fibroblasts, BMC Genomics 14 (2013 Apr 14) 224.